Comparison between the continuum threshold and the Polyakov loop as deconfinement order parameters

J. P. Carlomagno[1,2] and M. Loewe[3,4,5]

[1]*IFLP, CONICET—Dpto. de Física, Universidad Nacional de La Plata, C.C. 67, 1900 La Plata, Argentina*
[2]*CONICET, Rivadavia 1917, 1033 Buenos Aires, Argentina*
[3]*Instituto de Física, Pontificia Universidad Católica de Chile, Casilla 306, Santiago 22, Chile*
[4]*Centre for Theoretical and Mathematical Physics and Department of Physics, University of Cape Town, Rondebosch 7700, South Africa*
[5]*Centro Científico-Tecnológico de Valparaíso-CCTVAL, Universidad Técnica Federico Santa María, Valparaíso, Chile*

(Received 20 October 2016; published 7 February 2017)

We study the relation between the continuum threshold s_0 within finite energy sum rules and the trace of the Polyakov loop Φ in the framework of a nonlocal SU(2) chiral quark model, establishing a contact between both deconfinement order parameters at finite temperature T and chemical potential μ. In our analysis, we also include the order parameter for the chiral symmetry restoration, the chiral quark condensate. We found that s_0 and Φ provide us with the same information for the deconfinement transition, both for the zero and finite chemical potential cases. At zero density, the critical temperatures for both quantities coincide exactly and, at finite μ both order parameters provide evidence for the appearance of a quarkyonic phase.

DOI: 10.1103/PhysRevD.95.036003

I. INTRODUCTION

In QCD the strong interaction among quarks depends on their color charge. When quarks are placed in a medium, this color charge is screened due to density and temperature effects [1]. If the density and/or the temperature increases beyond a certain critical value, one expects that the interactions between quarks no longer confine them inside a hadron, so that they are free to travel longer distances and deconfine. This transition from a confined to a deconfined phase is usually referred to as the deconfinement phase transition.

A separate phase transition takes place when the realization of chiral symmetry shifts from a Nambu-Goldstone phase to a Wigner-Weyl phase. Based on lattice QCD evidence [2] one expects these two phase transitions to take place at approximately the same temperature at zero chemical potential. At finite density these two transitions can arise at different critical temperatures. The result will be a quarkyonic phase, where the chiral symmetry is restored but the quarks and gluons remain confined.

In order to characterize the properties of these phase transitions it has been customary to study the behavior of corresponding order parameters as functions of the temperature T and the baryon chemical potential μ, namely the trace of the Polyakov loop (PL) $\Phi(T,\mu)$ (deconfinement phase transition) and quark antiquark chiral condensate $\langle\bar{\psi}\psi\rangle(T,\mu)$ (chiral symmetry restoration), respectively.

Another important parameter in the discussion of these phase transitions is the role that an external magnetic field may play, inducing changes in the critical temperature, in the location of the critical endpoint, etc [3]. However, in this work we will not refer to magnetic field effects, since the goal of our discussion is to compare the Polyakov loop order parameter with another QCD deconfinement parameter that has been introduced in the literature [4] in the form of the squared energy threshold, $s_0(T,\mu)$, for the onset of perturbative QCD (PQCD) in hadronic spectral functions. For an actual general review see Ref. [5]. Around this energy, and at zero temperature, the resonance peaks in the spectrum are either no longer present or become very broad. The smooth hadronic spectral function thus approaches the PQCD regime. With increasing temperature approaching the critical temperature for deconfinement, one would expect hadrons to disappear from the spectral function which should then be described entirely by PQCD.

When both T and μ are nonzero, lattice QCD simulations cannot be used, because of the sign problem in the fermionic determinant. Therefore, one needs to resort either to mathematical constructions to overcome the above limitation, or to model calculations.

The two deconfinement order parameters mentioned before: $\Phi(T,\mu)$ and $s_0(T,\mu)$ can be used to realize a phenomenological description of the deconfinement transition at finite temperature and density.

The natural framework to determine s_0 has been that of QCD sum rules [6]. This quantum field theory framework is based on the operator product expansion (OPE) of current correlators at short distances, extended beyond perturbation theory, and on Cauchy's theorem in the complex s-plane. The latter is usually referred to as quark-hadron duality. Vacuum expectation values of quark and gluon field operators effectively parametrize the effects of confinement. An extension of this method to finite

temperature was first outlined in [4]. Further evidence supporting the validity of this program was provided in [7], followed by a large number of applications [8,9].

To analyze the role of the PL, we will concentrate on nonlocal Polyakov-Nambu-Jona-Lasinio (nlPNJL) models [10–15], in which quarks move in a background color field and interact through covariant nonlocal chirally symmetric four point couplings. These approaches, which can be considered as an improvement over the (local) PNJL model [16–22], offer a common framework to study both the chiral restoration and deconfinement transitions. In fact, the nonlocal character of the interactions arises naturally in the context of several successful approaches to low-energy quark dynamics [23–25], and leads to a momentum dependence in the quark propagator that can be made consistent [26] with lattice results [27–29].

In view of the above mentioned points, the aim of the present work is to study the relation between both order parameters for the deconfinement transition at finite temperature and chemical potential, Φ and s_0, using the thermal finite energy sum rules (FESR) with inputs obtained from nlPNJL models.

II. FINITE ENERGY SUM RULES

We begin by considering the (charged) axial-vector current correlator at $T = 0$

$$\Pi_{\mu\nu}(q^2) = i\int d^4x e^{iq\cdot x}\langle 0|T(A_\mu(x)A_\nu(0))|0\rangle, \\ = -g_{\mu\nu}\Pi_1(q^2) + q_\mu q_\nu \Pi_0(q^2), \quad (1)$$

where $A_\mu(x) =: \bar{u}(x)\gamma_\mu\gamma_5 d(x)$: is the axial-vector current, $q_\mu = (\omega, \vec{q})$ is the four-momentum transfer, and the functions $\Pi_{0,1}(q^2)$ are free of kinematical singularities. Concentrating on the function $\Pi_0(q^2)$ and writing the OPE beyond perturbation theory in QCD [6], one of the two pillars of the sum rule method, one has

$$\Pi_0(q^2)|_{\rm QCD} = C_0\hat{I} + \sum_{N=1} C_{2N}(q^2,\mu^2)\langle\hat{\mathcal{O}}_{2N}(\mu^2)\rangle, \quad (2)$$

where μ^2 is a renormalization scale. The Wilson coefficients C_N depend on the Lorentz indices and quantum numbers of the currents. Finally, the local gauge invariant operators $\hat{\mathcal{O}}_N$, are built from the quark and gluon fields in the QCD Lagrangian. The vacuum expectation values of those operators ($\hat{\mathcal{O}}_{2N}(\mu^2)$), dubbed as condensates, parametrize nonperturbative effects and have to be extracted from experimental data or model calculations. These operators are ordered by increasing dimensionality and the Wilson coefficients, calculable in PQCD, fall off by corresponding powers of $-q^2$. The unit operator above has dimension $d = 0$ and $C_0\hat{I}$ stands for the purely perturbative contribution. Hence, this OPE factorizes short distance physics, encapsulated in the Wilson coefficients, and long distance effects parametrized by the vacuum condensates.

The second pillar of the QCD sum rules technique is Cauchy's theorem in the complex squared energy s-plane

$$\frac{1}{\pi}\int_0^{s_0} ds f(s)\mathrm{Im}\Pi_0(s)|_{\rm HAD} \\ = -\frac{1}{2\pi i}\oint_{C(|s_0|)} ds f(s)\Pi_0(s)|_{\rm QCD}, \quad (3)$$

where $f(s)$ is an arbitrary analytic function, and the radius of the circle s_0 is large enough for QCD and the OPE to be used on the circle. The integral along the real s-axis involves the hadronic spectral function. This equation is the mathematical statement of what is usually referred to as quark-hadron duality. Using the OPE, Eq. (2), and an integration kernel $f(s) = s^N (N = 1, 2, \ldots)$ one obtains the FESR

$$(-)^{N-1}C_{2N}\langle\hat{\mathcal{O}}_{2N}\rangle = 4\pi^2\int_0^{s_0} ds s^{N-1}\frac{1}{\pi}\mathrm{Im}\Pi_0(s)|_{\rm HAD} \\ -\frac{s_0^N}{N}[1+\mathcal{O}(\alpha_s)](N = 1, 2, \ldots). \quad (4)$$

For $N = 1$, the dimension $d = 2$ term in the OPE does not involve any condensate, as it is not possible to construct a gauge invariant operator of such a dimension from the quark and gluon fields. There is no evidence for such a term (at $T = 0$) from FESR analyses of experimental data on e^+e^- annihilation and τ decays into hadrons [30,31]. At high temperatures, though, there seems to be evidence for some $d = 2$ term [32]. However, the analysis to be reported here is performed at lower values of T, so that we can safely ignore this contribution in the sequel.

The dimension $d = 4$ term, a renormalization group invariant quantity, is given by

$$C_4\langle\hat{\mathcal{O}}_4\rangle = \frac{\pi}{6}\langle\alpha_s G^2\rangle + 2\pi^2(m_u + m_d)\langle\bar{q}q\rangle. \quad (5)$$

The leading power correction of dimension $d = 6$ is the four-quark condensate, which in the vacuum saturation approximation [6] becomes

$$C_6\langle\hat{\mathcal{O}}_6\rangle = \frac{896}{81}\pi^3\alpha_s|\langle\bar{q}q\rangle|^2, \quad (6)$$

which has a very mild dependence on the renormalization scale. This approximation has no solid theoretical justification, other than its simplicity. Hence, there is no reliable way of estimating corrections, which in fact appear to be rather large from comparisons between Eq. (6) and direct determinations from data [31].

The extension of this program to finite temperature is fairly straightforward [4,7,33], with the Wilson coefficients

in the OPE, Eq. (2), remaining independent of T at leading order in α_s, and the condensates developing a temperature dependence. Radiative corrections in QCD involve now an additional scale, i.e. the temperature, so that $\alpha_s \equiv \alpha_s(\mu^2, T)$. This problem has not yet been solved successfully. Nevertheless, from the size of radiative corrections at $T = 0$ one does not expect any major loss of accuracy in results from thermal FESR to leading order in PQCD, as long as the temperature is not too high, say $T \lesssim 200$ MeV. Essentially all applications of FESR at $T \neq 0$ have been done at leading order in PQCD, thus implying a systematic uncertainty at the level of 10%.

In the static limit ($\vec{q} \to 0$), to leading order in PQCD, and for $T \neq 0$ and $\mu \neq 0$ the function $\Pi_0(q^2)|_{\rm QCD}$ in Eq. (1) becomes $\Pi_0(\omega^2, T, \mu)|_{\rm QCD}$; to simplify the notation we shall omit the T and μ dependence in the sequel. A straightforward calculation of the spectral function in perturbative QCD, at finite temperature and finite density gives

$$\frac{1}{\pi}\mathrm{Im}\Pi_0(s)|_{\rm PQCD} = \frac{1}{4\pi^2}\left[1 - \tilde{n}_+\left(\frac{\sqrt{s}}{2}\right) - \tilde{n}_-\left(\frac{\sqrt{s}}{2}\right)\right] - \frac{2}{\pi^2}T^2\delta(s)[\mathrm{Li}_2(-e^{\mu/T}) + \mathrm{Li}_2(-e^{-\mu/T})], \tag{7}$$

where $\mathrm{Li}_2(x)$ is the dilogarithm function, $s = \omega^2$, and

$$\tilde{n}_\pm(x) = \frac{1}{e^{(x\mp\mu)/T} + 1} \tag{8}$$

are the Fermi-Dirac thermal distributions for particles and antiparticles, respectively.

In the hadronic sector we assume pion-pole dominance of the hadronic spectral function, i.e. the continuum threshold s_0 to lie below the first radial excitation with mass $M_{\pi_1} \simeq 1300$ MeV. This is a very good approximation at finite T, as we expect s_0 to be monotonically decreasing with increasing temperature. In this case,

$$\frac{1}{\pi}\mathrm{Im}\Pi_0(s)|_{\rm HAD} = 2f_\pi^2(T, \mu_B)\delta(s - m_\pi^2), \tag{9}$$

where $f_\pi(T, \mu_B)$ is the pion decay constant at finite T and μ, with $f_\pi(0, 0) = 92.21 \pm 0.14$ MeV [34]. Notice we will not include in our spectral function the first part of a_1 resonance obtained from the τ-decay data [35], since still there is no counterpart in the SU(2) nlPNJL model for the description of the hadronic vector resonance. A zero temperature analysis has been done for the vector case in Ref. [36].

Turning to the FESR, Eq. (4), with $N = 1$ and no dimension $d = 2$ condensate, and using Eqs. (7) and (9) one finds

$$\int_0^{s_0(T,\mu)} ds\left[1 - \tilde{n}_+\left(\frac{\sqrt{s}}{2}\right) - \tilde{n}_-\left(\frac{\sqrt{s}}{2}\right)\right] = 8\pi^2 f_\pi^2(T, \mu) + 8T^2[\mathrm{Li}_2(-e^{\mu/T}) + \mathrm{Li}_2(-e^{-\mu/T})]. \tag{10}$$

This is a transcendental equation determining $s_0(T, \mu)$ in terms of $f_\pi(T, \mu)$.

For completeness, the other two thermal FESR at zero chemical potential are given by [35],

$$-C_4\langle\hat{\mathcal{O}}_4\rangle(T) = 4\pi^2\int_0^{s_0(T)} dss\frac{1}{\pi}\mathrm{Im}\Pi_0(s)|_{\rm HAD} - \int_0^{s_0(T)} dss\left[1 - 2n_F\left(\frac{\sqrt{s}}{2T}\right)\right], \tag{11}$$

$$C_6\langle\hat{\mathcal{O}}_6\rangle(T) = 4\pi^2\int_0^{s_0(T)} dss^2\frac{1}{\pi}\mathrm{Im}\Pi_0(s)|_{\rm HAD} - \int_0^{s_0(T)} dss^2[1 - 2n_F\left(\frac{\sqrt{s}}{2T}\right)], \tag{12}$$

where $n_F(x) = 1/(1 + e^x)$ is the Fermi thermal function.

III. THERMODYNAMICS AT FINITE DENSITY IN THE PNJL MODEL

We consider a nonlocal SU(2) chiral quark model that includes quark couplings to the color gauge fields. The corresponding Euclidean effective action is given by [37,38]

$$S_E = \int d^4x\{\bar{\psi}(x)(-i\gamma_\mu D_\mu + \hat{m})\psi(x) - \frac{G_S}{2}[j_a(x)j_a(x) - j_P(x)j_P(x)] + \mathcal{U}(\Phi[A(x)])\}, \tag{13}$$

where ψ is the $N_f = 2$ fermion doublet $\psi \equiv (u, d)^T$, G_S is the coupling parameter for the interaction terms and $\hat{m} = \mathrm{diag}(m_u, m_d)$ is the current quark mass matrix. In what follows we consider isospin symmetry, $m_u = m_d = m$. The fermion kinetic term in Eq. (13) includes a covariant derivative $D_\mu \equiv \partial_\mu - iA_\mu$, where A_μ are color gauge fields. The nonlocal currents $j_a(x), j_P(x)$ are given by

$$j_a(x) = \int d^4z\mathcal{G}(z)\bar{\psi}\left(x + \frac{z}{2}\right)\Gamma_a\psi\left(x - \frac{z}{2}\right),$$
$$j_P(x) = \int d^4z\mathcal{F}(z)\bar{\psi}\left(x + \frac{z}{2}\right)\frac{i\overleftrightarrow{\not\partial}}{2\kappa_p}\psi\left(x - \frac{z}{2}\right), \tag{14}$$

where, $\Gamma_a = (\mathbb{1}, i\gamma_5\vec{\tau})$ and $u(x')\overleftrightarrow{\partial}v(x) = u(x')\partial_x v(x) - \partial_{x'}u(x')v(x)$. The functions $\mathcal{G}(z)$ and $\mathcal{F}(z)$ in Eq. (14)

are nonlocal covariant form factors characterizing the corresponding interactions.

Notice that the four currents $j_a(x)$ require a common form factor $\mathcal{G}(z)$ in order to guarantee chiral invariance, while the coupling $j_P(x)j_P(x)$ is self-invariant under chiral transformations. The relative weight of the interaction driven by $j_P(x)$ is controlled by the parameter κ_p. The scalar-isoscalar component of the $j_a(x)$ current will generate a momentum dependent quark mass in the quark propagator, while the "momentum" current $j_P(x)$ will be responsible for a momentum dependent quark wave function renormalization (WFR) [26,37,38]. If is not included, the mass parameter in the quark propagator cannot be compare with lattice results.

Now we perform a bosonization of the theory, introducing bosonic fields $\sigma_{1,2}(x)$ and $\pi_a(x)$, and integrating out the quark fields. Details of this procedure can be found e.g. in Ref. [26].

In order to analyze the properties of meson fields it is necessary to consider the quadratic fluctuations in the Euclidean action:

$$S_E^{\text{quad}} = \frac{1}{2}\int \frac{d^4p}{(2\pi)^4}\sum_M r_M G_M(p^2)\phi_M(p)\bar{\phi}_M(-p), \tag{15}$$

where meson fluctuations $\delta\sigma_a, \delta\pi_a$ have been translated to a charged basis ϕ_M, being M the scalar and pseudoscalar mesons $(\sigma, \pi^0, \pi^\pm)$ plus the σ_2 field, and G_M are the inverse dressed propagators. The coefficient r_M is 1 for charge eigenstates $M = \sigma_i, \pi^0$, and 2 for $M = \pi^+$. Meson masses are then given by the equations

$$G_M(-m_M^2) = 0, \tag{16}$$

where the full expressions for the one-loop functions $G_M(q)$ can be found in Ref. [15,26]. In addition, physical states have to be normalized through

$$\tilde{\phi}_M(p) = Z_M^{-1/2}\phi_M(p), \tag{17}$$

where

$$Z_M^{-1} = \left.\frac{dG_M(p)}{dp^2}\right|_{p^2=-m_M^2}. \tag{18}$$

At finite temperature, the meson masses are obtained by solving $G_M(-m_M^2, \vec{0}) = 0$. The mass values determined by these equations are the spatial "screening-masses" corresponding to the zeroth Matsubara mode, and their inverses describe the persistence lengths of these modes at equilibrium with the heat bath [12].

At zero temperature, one can also calculate the weak decay constants of pseudoscalar mesons. These are given by the matrix elements of the axial currents A_μ^a between the vacuum and the physical meson states,

$$\imath f_{ab}(p^2)p_\mu = \langle 0|A_\mu^a(0)|\delta\pi_b(p)\rangle. \tag{19}$$

The matrix elements can be calculated from the expansion of the Euclidean effective action in the presence of external axial currents,

$$\langle 0|A_\mu^a(0)|\delta\pi_b(p)\rangle = \left.\frac{\delta^2 S_E}{\delta A_\mu^a \delta\pi_b(p)}\right|_{A_\mu^a=\delta\pi_b=0}, \tag{20}$$

Performing the derivative of the resulting expressions with respect to the renormalized meson fields, we can finally identify the corresponding pion weak decay constant [15,26]

$$f_\pi = \frac{mZ_\pi^{-1/2}}{m_\pi^2}F_0(-m_\pi^2) \tag{21}$$

with

$$F_0(p^2) = 8N_c\int\frac{d^4q}{(2\pi)^4}g(q)\frac{Z(q^+)Z(q^-)}{D(q^+)D(q^-)} \times [q^+\cdot q^- + M(q^+)M(q^-)] \tag{22}$$

where $q^\pm = q \pm p/2$ and $D(q) = q^2 + M^2(q)$, with $M(p)$ and $Z(p)$ defined as

$$M(p) = Z(p)[m + \bar{\sigma}_1 g(p)],$$
$$Z(p) = [1 - \bar{\sigma}_2 f(p)]^{-1}. \tag{23}$$

Here $g(p)$ and $f(p)$ are the Fourier transforms of the form factors in Eq. (14).

Since we are interested in the deconfinement and chiral restoration critical temperatures, we extend the bosonized effective action to finite temperature T and chemical potential μ. This will be done using the standard imaginary time formalism. Concerning the gauge fields A_μ, we assume that quarks move on a constant background field $\phi = A_4 = iA_0 = ig\delta_{\mu 0}G_a^\mu\lambda^a/2$, where G_a^μ are SU(3) color gauge fields. Then the traced Polyakov loop, which in the infinite quark mass limit can be taken as an order parameter of confinement, is given by $\Phi = \frac{1}{3}\text{Tr}\exp(i\phi/T)$. For the light quark sector the trace of the Polyakov loop turns out to be an approximate order parameter in the same way the chiral quark condensate is an approximate order parameter for the chiral symmetry restoration outside the chiral limit. We work in the so-called Polyakov gauge [39], where the matrix ϕ is given a diagonal representation $\phi = \phi_3\lambda_3 + \phi_8\lambda_8$.

The introduction of the Polyakov loop formally leads to a complex valued action at nonzero chemical potential.

Even for a complex Euclidean action, one can still search for the configuration with the largest weight in the path integral and refer to this as the mean field configuration. One way to establish such a lowest order approximation is to use the real part of the thermodynamic potential in the mean field equations.

The thermal expectation values $\langle\Phi\rangle$ and $\langle\Phi^*\rangle$ of the conjugate Polyakov loop fields must be real quantities [20,40], this means $\Phi = \Phi^*$ for the mean field configurations. With the constraint of ϕ_3 and ϕ_8 being real, due to the connection to the QCD color gauge group, implies $\phi_8 = 0$, leaving only ϕ_3 as an independent variable, and therefore $\Phi = [2\cos(\phi_3/T) + 1]/3$.

With the above definition, the Polyakov loop expectation values $\langle\Phi\rangle$ and $\langle\Phi^*\rangle$ turn out to be equal in this limit, given the reality constraint on the thermodynamical potential in the mean field approximation $\Omega^{\rm MFA}$. The corrections beyond mean field for $\mathrm{Im}\Omega$, induced by the temporal gauge fields, cause the splitting between $\langle\Phi\rangle$ and $\langle\Phi^*\rangle$ [20,41,42].

Following the same prescriptions as in previous works, see e.g. Refs. [43,44], the real part of $\Omega^{\rm MFA}$ at finite temperature T and chemical potential μ is given by

$$\Omega^{\rm MFA} = \Omega^{\rm reg} + \Omega^{\rm free} + \mathcal{U}(\Phi, T) + \Omega_0, \tag{24}$$

where

$$\Omega^{\rm reg} = -4T \sum_{c=r,g,b} \sum_{n=-\infty}^{\infty} \int \frac{d^3\vec{p}}{(2\pi)^3} \log\left[\frac{(\rho^c_{n,\vec{p}})^2 + M^2(\rho^c_{n,\vec{p}})}{Z^2(\rho^c_{n,\vec{p}})}\right] + \frac{\bar{\sigma}_1^2 + \kappa_p^2\bar{\sigma}_2^2}{2G_S},$$
$$\Omega^{\rm free} = -4T \int \frac{d^3\vec{p}}{(2\pi)^3} \sum_{c=r,g,b} \sum_{s=\pm 1} \mathrm{Re}\log\left[1 + \exp\left(-\frac{\epsilon_p + is\phi_c}{T}\right)\right], \tag{25}$$

here $\bar{\sigma}_{1,2}$ are the mean field values of the scalar fields. We have also defined

$$(\rho^c_{n,\vec{p}})^2 = [(2n+1)\pi T + \phi_c - \imath\mu]^2 + \vec{p}^2, \tag{26}$$

the sums over color indices run over $c = r, g, b$, with the color background fields components being $\phi_r = -\phi_g = \phi_3$, $\phi_b = 0$, and $\epsilon_p = \sqrt{\vec{p}^2 + m^2}$. The term $\Omega^{\rm reg}$ is the regularized expression for the thermodynamical potential of a free fermion gas, and finally the last term in Eq. (24) is just a constant fixed by the condition that $\Omega^{\rm MFA}$ vanishes at $T = \mu = 0$.

The effective gauge field self-interactions are given by the Polyakov loop potential $\mathcal{U}(\Phi, T)$. At finite temperature T, it is usual to take for this potential a functional form based on properties of pure gauge QCD. One possible Ansatz is that based on the logarithmic expression of the Haar measure associated with the SU(3) color group integration. The corresponding potential is given by [20]

$$\frac{\mathcal{U}_{\log}(\Phi, T)}{T^4} = -\frac{1}{2}a(T)\Phi^2 + b(T)\log(1 - 6\Phi^2 + 8\Phi^3 - 3\Phi^4), \tag{27}$$

where

$$a(T) = a_0 + a_1\left(\frac{T_0}{T}\right) + a_2\left(\frac{T_0}{T}\right)^2,$$
$$b(T) = b_3\left(\frac{T_0}{T}\right)^3. \tag{28}$$

The parameters can be fitted to pure gauge lattice QCD data to properly reproduce the corresponding equation of state and the Polyakov loop behavior [20]. The values of a_i and b_i are constrained by the condition of reaching the Stefan-Boltzmann limit at $T \to \infty$ and by imposing the presence of a first-order phase transition at T_0, which is a further parameter of the model. At the critical temperature, the Polyakov loop potential develops a second degenerate minimum giving raise to a first order phase transition.

In the absence of dynamical quarks, from lattice calculations one expects a deconfinement temperature $T_0 = 270$ MeV. However, it has been argued that in the presence of light dynamical quarks this temperature scale should be adequately reduced to about 210 and 190 MeV for the case of two and three flavors, respectively, with an uncertainty of about 30 MeV [45]. In this work we will use $T_0 = 208$ MeV.

Besides the logarithmic function in Eq. (27), a widely used potential is that given by a polynomial function based on a Ginzburg-Landau Ansatz [19,46]:

$$\frac{\mathcal{U}_{\rm poly}(\Phi, T)}{T^4} = -\frac{b_2(T)}{2}\Phi^2 - \frac{b_3}{3}\Phi^3 + \frac{b_4}{4}\Phi^4, \tag{29}$$

where

$$b_2(T) = a_0 + a_1\left(\frac{T_0}{T}\right) + a_2\left(\frac{T_0}{T}\right)^2 + a_3\left(\frac{T_0}{T}\right)^3. \tag{30}$$

Once again, the parameters can be fitted to pure gauge lattice QCD results to reproduce the corresponding equation of state and Polyakov loop behavior (numerical values can be found in Ref. [19]).

TABLE I. Set of model parameters for the form factors in Eqs. (32), (13), (14).

	Set
m [MeV]	5.7
$G\Lambda_0^2$	32.02
κ_p [GeV]	4.17
Λ_0 [GeV]	0.814
Λ_1 [GeV]	1.033

Given the full form of the thermodynamical potential, the mean field values $\bar{\sigma}_{1,2}$ and ϕ_3 can be obtained as solutions of the coupled set of gap equations

$$\frac{\partial\Omega_{\rm reg}^{\rm MFA}}{(\partial\sigma_1,\partial\sigma_2,\partial\phi_3)}=0. \tag{31}$$

In order to fully specify the model under consideration, we proceed to fix the model parameters as well as the nonlocal form factors $g(q)$ and $f(q)$. We consider here Gaussian functions

$$\begin{aligned} g(q)&=\exp\left(-q^2/\Lambda_0^2\right),\\ f(q)&=\exp\left(-q^2/\Lambda_1^2\right), \end{aligned} \tag{32}$$

which guarantee a fast ultraviolet convergence of the loop integrals. The values of the five free parameters are summarized in Table I and can be found in Ref. [26].

Once the mean field values are obtained, the behavior of other relevant quantities as functions of the temperature and chemical potential can be determined. We concentrate, in particular, on the chiral quark condensate $\langle\bar{q}q\rangle=\partial\Omega_{\rm reg}^{\rm MFA}/\partial m$ and the traced Polyakov loop Φ, which will be taken as order parameters for the chiral restoration and deconfinement transitions, respectively. The associated susceptibilities will be defined as $\chi_{\rm ch}=\partial\langle\bar{q}q\rangle/\partial m$ and $\chi_{\rm PL}=d\Phi/dT$.

In Ref [2], the deconfinement temperature, defined at the peak of the entropy of a static quark (which is related to the Polyakov loop) is located at the same temperature, within errors, as the chiral susceptibility even at finite lattice spacing.

In several works (see [2] and references therein), the deconfinement transition in lattice QCD with light dynamical quarks has been studied in terms of the inflection point of the renormalized Polyakov loop and fluctuations of conserved charges. Usually, the critical deconfinement temperatures are equal or larger than the restoring chiral transition critical temperature. Nevertheless, these approaches have the disadvantage of being lattice scheme dependent and therefore the obtained values may differ considerably between them.

In this work we define the deconfinement transition temperature, in the crossover region, with the peak of the Polyakov susceptibility $\chi_{\rm PL}$, which turns out to be equivalent to the susceptibility of the free energy of a static quark. In the region where the deconfinement is a first order phase transition we use the same prescription as Ref. [37], where the critical temperature is defined as the temperature where $\Phi=0.4$.

IV. RESULTS

In order to determine the relation between both order parameters for the deconfinement transition, namely the perturbative QCD threshold s_0 and the trace of the Polyakov loop Φ as functions of the temperature and chemical potential we begin our analysis studying the finite energy sum rules at zero density. In this scenario, when $\mu=0$, the Eq. (10) becomes

$$8\pi^2 f_\pi^2(T)=\frac{4}{3}\pi^2T^2+\int_0^{s_0(T)}ds\left[1-2n_F\left(\frac{\sqrt{s}}{2T}\right)\right], \tag{33}$$

where the pion decay constant at finite temperature and/or chemical potential is calculated using Eq. (21) and Eq. (22) as

$$\begin{aligned} F_0(p^2)=8T\sum_{c,n}\int\frac{d^3\vec{q}}{(2\pi)^4}g(\rho^c_{n,\vec{q}})\frac{Z(\rho^{c}_{n,\vec{q}}{}^{+})Z(\rho^{c}_{n,\vec{q}}{}^{-})}{D(\rho^{c}_{n,\vec{q}}{}^{+})D(\rho^{c}_{n,\vec{q}}{}^{-})}\\ \times\left[\rho^{c}_{n,\vec{q}}{}^{+}\cdot\rho^{c}_{n,\vec{q}}{}^{-}+M(\rho^{c}_{n,\vec{q}}{}^{+})M(\rho^{c}_{n,\vec{q}}{}^{-})\right] \end{aligned} \tag{34}$$

where $\rho^{c}_{n,\vec{q}}{}^{\pm}=\rho^c_{n,\vec{q}}\pm p/2$.

It is known that in local versions of the PNJL model, at zero chemical potential, the restoration of the chiral symmetry and the deconfinement transition take place at different temperatures (see e.g. Refs. [47,48]), usually separated by approximate 20 MeV. Therefore, it is interesting to analyze the results obtained in a nonlocal and in a local PNJL model, the latter one parametrized according to [19]. In Fig. 1 we plot the continuum threshold, the trace of the PL and the normalized quark condensate for the nonlocal (local) PNJL model in thick (thin) line, for the logarithmic and polynomial effective potentials. As we expected from previous results, in the local version both transitions do not occur simultaneously. In this scenario, the PQCD threshold vanishes at a critical temperature, $T_c^{s_0}$, located between the chiral critical temperature T_c^{χ} and the PL deconfinement temperature T_c^{Φ} (obtained through the corresponding susceptibilities).

In the case of the nonlocal PNJL model, for both effective potentials, s_0 and Φ have a similar critical temperature for the deconfinement transition of approximate $T_c\sim 170$ MeV. These temperatures are summarized in Table II.

The value obtained at zero temperature for the continuum threshold, $s_0\sim 670$, MeV is rather small but in a good agreement with other calculations in sum rules using

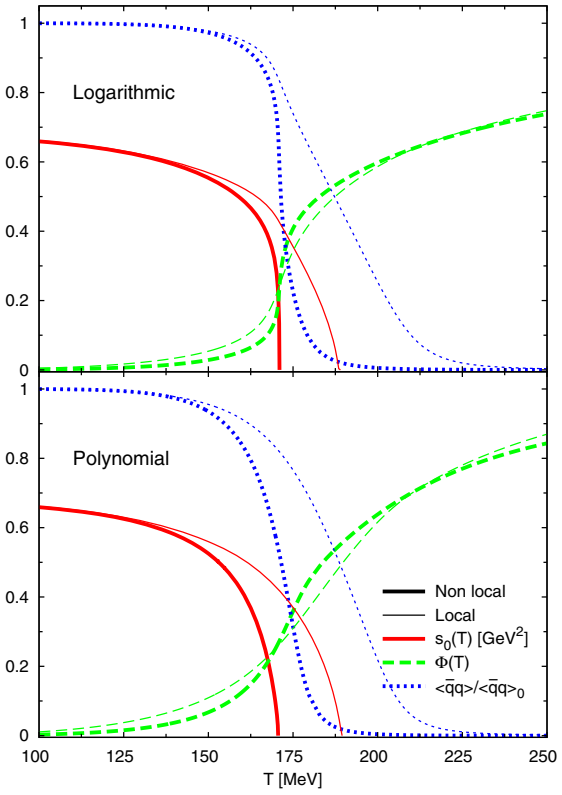

FIG. 1. Continuum threshold (red solid line), trace of the Polyakov loop (green dashed line) and the normalized quark condensate (blue dotted line) as a function of the temperature for nonlocal (thick line) and local PNJL model (thin line) at zero chemical potential for logarithmic (upper panel) and polynomial (lower panel) effective potentials.

as input LQCD results. The main reason for this lower value is the pion pole approximation for the spectral function. When additional information is incorporated, for instance the a_1 resonance, the value of $s_0(T=0)$ increases substantially [35].

Just for completeness and, in addition to the main goal of this article, from the higher order FESR, Eqs. (11) and (12), we can estimate the gluon condensate and the four-quark condensate. The former shows the expected behavior with a finite value at zero temperature. It decreases monotonically as function of temperature, vanishing at $T \sim 170$ MeV. A recent calculation of this quantity can be found in Ref. [49],

TABLE II. Chiral critical temperatures T_c^{χ}, deconfinement temperatures T_c^{Φ} and $T_c^{s_0}$ for the local and nonlocal PNJL model with logarithmic and polynomial effective potentials.

	Logarithmic		Polynomial	
	Nonlocal	Local	Nonlocal	Local
T_c^{χ} [MeV]	171	205	176	201
T_c^{Φ} [MeV]	171	171	174	183
$T_c^{s_0}$ [MeV]	171	189	170	190

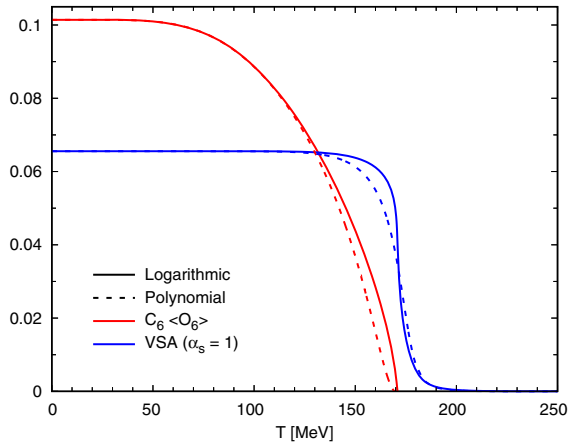

FIG. 2. Four-quark condensate in the vacuum saturation approximation with $\alpha_s = 1$ [51] (blue line) and $C_6\langle\hat{\mathcal{O}}_6\rangle$ (red line) for the logarithmic (polynomial) Polyakov effective potential in solid (dashed) line, at zero density as a function of the temperature.

determined from e^+e annihilation data in the charm-quark region. The four quark condensate, plotted in Fig. 2, was compared, according to the vacuum saturation approximation (VSA), with the squared of the chiral quark condensate obtained within the $SU(2)$ nlPNJL model. If we assume that the previous approximation is exact, from Eqs. (6) and (12), at zero temperature and in the chiral limit, we obtain that $\alpha_s = \frac{108\pi^3}{7}\frac{f_\pi^6}{|\langle\bar{q}q\rangle|^2} \simeq 1.6$ (a very similar result is obtained outside the chiral limit), meaning that the VSA underestimate $C_6\langle\hat{\mathcal{O}}_6\rangle$. This value is considerably higher than recent estimations of the strong coupling at low energies, based on completely different approaches [50,51]. The first one relies on a recent analysis of the ALEPH data for the τ decay, whereas the second one corresponds to a general recent review including different perspectives.

From Fig. 2, we see that for both Polyakov effective potentials, the VSA is about 40% less than the four-quark condensate obtained from FESR at zero temperature, in qualitatively agreement with estimates, based on $K^0 - \bar{K}^0$ mixing [52].

From lattice QCD calculations, at zero chemical potential, the chiral symmetry restoration and the deconfinement transition take place at the same critical temperature. This behavior was verified in nlPNJL models [15,37] and also obtained by finite energy sum rules [33]. The next natural step is to extend our analysis to a finite density scenario, to identify the relation between $s_0(T,\mu)$ and $\Phi(T,\mu)$.

In Fig. 3 we plot, for the logarithmic Polyakov effective potential, the normalized quark condensate $\langle\bar{q}q\rangle/\langle\bar{q}q\rangle_0$, the trace of the PL Φ and the continuum threshold s_0 as functions of the temperature for three different values of chemical potential. In the middle panel we choose $\mu = 139$ MeV, which corresponds to the critical endpoint chemical potential $\mu_{\rm CEP}$. For values of μ smaller than $\mu_{\rm CEP}$,

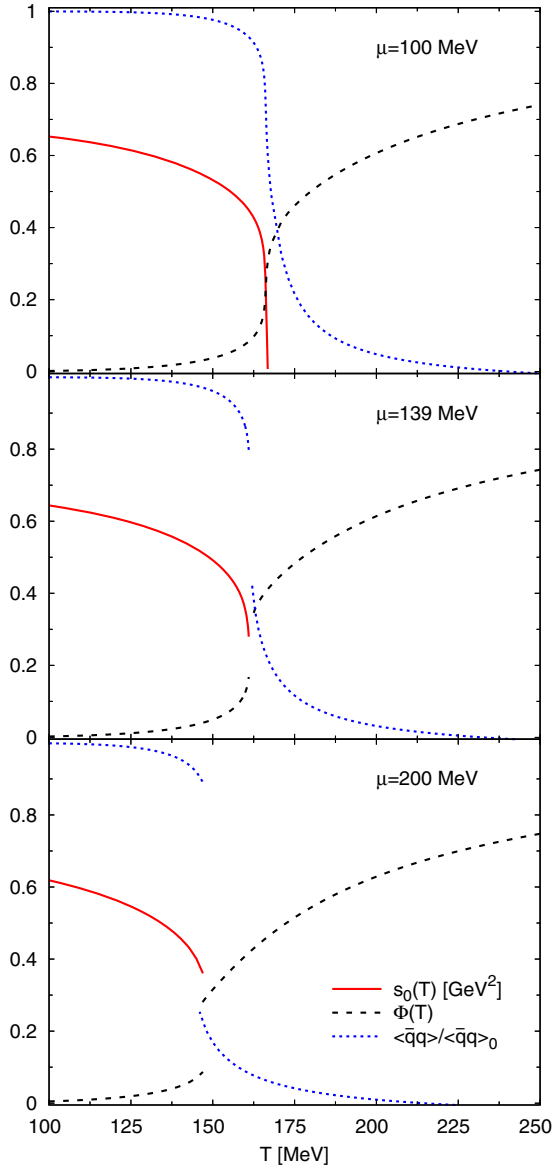

FIG. 3. Continuum threshold (solid red line), trace of the Polyakov loop (black dashed lined) and the normalized quark condensate (blue dotted line) as a function of the temperature at a constant density for the logarithmic effective potential.

the chiral restoration arises via a crossover transition. Beyond this critical density, a first order phase transition occurs. This value, together with the critical temperature $T_{\mathrm{CEP}} = 161$ MeV determines the coordinates of the critical endpoint.

All the results presented here were obtained by Gaussian regulators [see Eq. (32)]. For instance, if we would have chosen a Lorentzian regulator [15] for the form factors, inspired by lattice results, or if the momentum current would have been neglected, which means that no WFR effects would be present [12], similar outcomes would have been found. It turns out that the chiral and deconfinement critical temperatures get a minor dependence on the explicit shape used to parametrize the form factors [38,53].

In the upper panel of Fig. 3, where $\mu = 100$ MeV, we see that the chiral and deconfinement transitions are crossovers occurring at the same critical temperature. The peak of the Polyakov susceptibility and the point where the continuum threshold vanishes occur at approximate the same temperature $T_c \sim 166$ MeV.

When μ becomes equal or higher than $\mu = 139$ MeV, the order parameter for the chiral symmetry restoration has a discontinuity signaling a first order phase transition. This gap in the quark condensate induces also a jump in the trace of the PL (see middle and lower panels in Fig. 3). The value of Φ at the discontinuity indicates that at this temperature the system remains confined but in a chiral symmetry restored state. This region is usually referred as the quarkyonic phase [54–56].

At bigger densities than the critical endpoint chemical potential, the thermal equation has not solution beyond the critical temperature. The term proportional to the dilogarithm becomes too negative and therefore Eq. (10) cannot be satisfied. The continuum threshold stops with a finite value at the chiral critical temperature (see middle and lower panels in Fig. 3). We see in this way, that the Polyakov loop and the continuum threshold provide the same information. When the chiral symmetry is restored, s_0 and Φ show that we are still in a confined phase. This characterizes the occurrence of a quarkyonic phase.

V. SUMMARY AND CONCLUSIONS

In this article we discuss if the behavior of two vastly used order parameters for the deconfinement transition: the continuum threshold and the trace of the Polyakov loop, provide us with the same physical insight.

To accomplish this analysis, we use finite energy sum rules for the axial-vector current correlator. In this framework, one can define the continuum threshold as the energy where the resonance peaks in the spectrum become very broad.

On the other side, the Polyakov loop is a thermal Wilson loop, gauge-invariant under the center of the color group which is expected to vanish in the confined phase and being different from zero in the deconfined phase.

The idea was to carry on the FESR program saturating the spectral function with the pion pole approximation. The input parameters we used in the spectral function, namely the pion mass, the pion decay constant and the chiral quark condensate, were obtained from a nonlocal SU(2) Polyakov-NJL model with Gaussian form factors. In this way we establish the connection between both approaches.

At zero density, we compare the trace of the Polyakov loop and the continuum threshold for the local and the nonlocal version of a PNJL model. We determine, for the nlPNJL model, that the continuum threshold vanishes at

the same temperature where the Polyakov susceptibility has its maximum value. In the case of the local PNJL, s_0 becomes zero between the critical temperature for the deconfinement transition, according to the Polyakov loop analysis, and the chiral restoration temperature.

At finite chemical potential, we find that for both deconfinement parameters, beyond the critical endpoint chemical potential, the system remains in its confined phase even when the chiral symmetry is restored. This is an evidence for the appearance of a quarkyonic phase.

We may conclude saying that our analysis gives strong support to the idea that both deconfinement parameters, in fact, provide the same kind of physical information.

ACKNOWLEDGMENTS

This work has been partially funded by CONICET (Argentina) under Grant No. PIP 449; by the National University of La Plata (Argentina), Project No. X718; by FONDECYT (Chile), under Grants No. 1130056, No. 1150171 and No. 1150847; and by Conicyt PIA/Basal Fb0821 (Chile). The authors would like to thank D. Gomez Dumm and N. N. Scoccola for useful discussions.

[1] K. Fukushima and T. Hatsuda, The phase diagram of dense QCD, Rep. Prog. Phys. **74**, 014001 (2011).

[2] A. Bazavov, N. Brambilla, H.-T. Ding, P. Petreczky, H.-P. Schadler, A. Vairo, and J. H. Weber, Polyakov loop in $2+1$ flavor QCD from low to high temperatures, Phys. Rev. D **93**, 114502 (2016).

[3] V. A. Miransky and I. A. Shovkovy, Quantum field theory in a magnetic field: From quantum chromodynamics to graphene and Dirac semimetals, Phys. Rep. **576**, 1 (2015).

[4] A. I. Bochkarev and M. E. Shaposhnikov, Hadronic mass scales and phase transitions in QCD, Nuovo Cimento Soc. Ital. Fis. **92A**, 17 (1986).

[5] Alejandro Ayala, C. A. Dominguez, and M. Loewe, QCD sum rules at finite temperature: A review, arXiv: 1608.04284.

[6] For a review see e.g. P. Colangelo and A. Khodjamirian, in *At the Frontier of Particle Physics/Handbook of QCD*, edited by M. Shifman (World Scientific, Singapore 2001), Vol. 3, p. 1495.

[7] C. A. Dominguez and M. Loewe, Comment on current correlators in QCD at finite temperature, Phys. Rev. D **52**, 3143 (1995).

[8] C. A. Dominguez and M. Loewe, Deconfinement and chiral-symmetry restoration at finite temperature, Phys. Lett. B **233**, 201 (1989); The (near) equality of the critical temperatures
for chiral-symmetry restoration and deconfinement was shown analytically in A. Barducci, R. Casalbuoni, S. De Curtis, R. Gatto, and G. Pettini, Heuristic argument for coincidence or almost coincidence of deconfinement and chirality restoration in finite temperature QCD, Phys. Lett. B **244**, 311 (1990).

[9] For recent applications see e.g. C. A. Dominguez, M. Loewe, and J. C. Rojas, Heavy-light quark pseudoscalar and vector mesons at finite temperature, J. High Energy Phys. 08 (2007) 040; C. A. Dominguez, M. Loewe, J. C. Rojas, and Y. Zhang, Charmonium in the vector channel at finite temperature from QCD sum rules, Phys. Rev. D **81**, 014007 (2010); (Pseudo)scalar charmonium in finite temperature QCD, Phys. Rev. D **83**, 034033 (2011), and references therein

[10] D. Blaschke, M. Buballa, A. E. Radzhabov, and M. K. Volkov, Effects of mesonic correlations in the QCD phase transition, Yad. Fiz. **71**, 2012 (2008) [Phys. At. Nucl. **71**, 1981 (2008)].

[11] G. A. Contrera, D. Gomez Dumm, and N. N. Scoccola, Nonlocal SU(3) chiral quark models at finite temperature: The Role of the Polyakov loop, Phys. Lett. B **661**, 113 (2008).

[12] G. A. Contrera, D. Gomez Dumm, and N. N. Scoccola, Meson properties at finite temperature in a three flavor nonlocal chiral quark model with Polyakov loop, Phys. Rev. D **81**, 054005 (2010).

[13] T. Hell, S. Roessner, M. Cristoforetti, and W. Weise, Dynamics and thermodynamics of a nonlocal PNJL model with running coupling, Phys. Rev. D **79**, 014022 (2009).

[14] T. Hell, S. Rossner, M. Cristoforetti, and W. Weise, Thermodynamics of a three-flavor nonlocal Polyakov-Nambu-Jona-Lasinio model, Phys. Rev. D **81**, 074034 (2010).

[15] J. P. Carlomagno, D. Gomez Dumm, and N. N. Scoccola, Deconfinement and chiral restoration in nonlocal SU(3) chiral quark models, Phys. Rev. D **88**, 074034 (2013).

[16] P. N. Meisinger and M. C. Ogilvie, Chiral symmetry restoration and Z(N) symmetry, Phys. Lett. B **379**, 163 (1996).

[17] K. Fukushima, Chiral effective model with the Polyakov loop, Phys. Lett. B **591**, 277 (2004).

[18] E. Megias, E. Ruiz Arriola, and L. L. Salcedo, Polyakov loop in chiral quark models at finite temperature, Phys. Rev. D **74**, 065005 (2006).

[19] C. Ratti, M. A. Thaler, and W. Weise, Phases of QCD: Lattice thermodynamics and a field theoretical model, Phys. Rev. D **73**, 014019 (2006).

[20] S. Roessner, C. Ratti, and W. Weise, Polyakov loop, diquarks and the two-flavour phase diagram, Phys. Rev. D **75**, 034007 (2007).

[21] S. Mukherjee, M. G. Mustafa, and R. Ray, Thermodynamics of the PNJL model with nonzero baryon and isospin chemical potentials, Phys. Rev. D **75**, 094015 (2007).

[22] C. Sasaki, B. Friman, and K. Redlich, Susceptibilities and the phase structure of a chiral model with Polyakov loops, Phys. Rev. D **75**, 074013 (2007).

[23] T. Schafer and E. V. Shuryak, Instantons in QCD, Rev. Mod. Phys. **70**, 323 (1998).
[24] C. D. Roberts and A. G. Williams, Dyson-Schwinger equations and their application to hadronic physics, Prog. Part. Nucl. Phys. **33**, 477 (1994).
[25] C. D. Roberts and S. M. Schmidt, Dyson-Schwinger equations: Density, temperature and continuum strong QCD, Prog. Part. Nucl. Phys. **45**, S1 (2000).
[26] S. Noguera and N. N. Scoccola, Nonlocal chiral quark models with wavefunction renormalization: Sigma properties and pi—pi scattering parameters, Phys. Rev. D **78**, 114002 (2008).
[27] P. O. Bowman, U. M. Heller, and A. G. Williams, Lattice quark propagator with staggered quarks in Landau and Laplacian gauges, Phys. Rev. D **66**, 014505 (2002); P. O. Bowman, U. M. Heller, D. B. Leinweber, and A. G. Williams, Modeling the quark propagator, Nucl. Phys. B, Proc. Suppl. **119**, 323 (2003).
[28] M. B. Parappilly, P. O. Bowman, U. M. Heller, D. B. Leinweber, A. G. Williams, and J. B. Zhang, Scaling behavior of quark propagator in full QCD, Phys. Rev. D **73**, 054504 (2006).
[29] S. Furui and H. Nakajima, Unquenched Kogut-Susskind quark propagator in lattice Landau gauge QCD, Phys. Rev. D **73**, 074503 (2006).
[30] C. A. Dominguez and K. Schilcher, Is there evidence for dimension two corrections in QCD two point functions?, Phys. Rev. D **61**, 114020 (2000).
[31] C. A. Dominguez and K. Schilcher, QCD vacuum condensates from tau-lepton decay data, J. High Energy Phys. 01 (2007) 093.
[32] E. Megias, E. Ruiz Arriola, and L. L. Salcedo, Correlations between perturbation theory and power corrections in QCD at zero and finite temperature, Phys. Rev. D **81**, 096009 (2010).
[33] Alejandro Ayala, A. Bashir, C. A. Dominguez, E. Gutierrez, M. Loewe, and A. Raya, QCD phase diagram from finite energy sum rules, Phys. Rev. D **84**, 056004 (2011).
[34] K. A. Olive *et al.* (Particle Data Group Collaboration), Review of particle physics, Chin. Phys. C **38**, 090001 (2014).
[35] C. A. Dominguez, M. Loewe, and Y. Zhang, Chiral symmetry restoration and deconfinement in QCD at finite temperature, Phys. Rev. D **86**, 034030 (2012); Erratum, Phys. Rev. D **90**, 039903(E) (2014).
[36] M. F. Izzo Villafae, D. Gomez Dumm, and N. N. Scoccola, Vector and axial vector mesons in a nonlocal chiral quark model, Phys. Rev. D **94**, 054003 (2016).
[37] G. A. Contrera, M. Orsaria, and N. N. Scoccola, Nonlocal Polyakov-Nambu-Jona-Lasinio model with wavefunction renormalization at finite temperature and chemical potential, Phys. Rev. D **82**, 054026 (2010).
[38] V. Pagura, D. Gomez Dumm, and N. N. Scoccola, Deconfinement and chiral restoration in nonlocal PNJL models at zero and imaginary chemical potential, Phys. Lett. B **707**, 76 (2012).
[39] D. Diakonov and M. Oswald, Gauge invariant effective action for the Polyakov line in the SU(N) Yang-Mills theory at high temperatures, Phys. Rev. D **70**, 105016 (2004).
[40] A. Dumitru, R. D. Pisarski, and D. Zschiesche, Dense quarks, and the fermion sign problem, in a SU(N) matrix model, Phys. Rev. D **72**, 065008 (2005).
[41] C. Ratti, S. Roessner, M. A. Thaler, and W. Weise, Thermodynamics of the PNJL model, Eur. Phys. J. C **49**, 213 (2007).
[42] C. Ratti, S. Roessner, and W. Weise, Quark number susceptibilities: Lattice QCD versus PNJL model, Phys. Lett. B **649**, 57 (2007).
[43] D. Gomez Dumm and N. N. Scoccola, Characteristics of the chiral phase transition in nonlocal quark models, Phys. Rev. C **72**, 014909 (2005).
[44] D. Gomez Dumm and N. N. Scoccola, Chiral quark models with nonlocal separable interactions at finite temperature and chemical potential, Phys. Rev. D **65**, 074021 (2002).
[45] B. J. Schaefer, J. M. Pawlowski, and J. Wambach, The phase structure of the Polyakov–quark-meson model, Phys. Rev. D **76**, 074023 (2007).
[46] O. Scavenius, A. Dumitru, and J. T. Lenaghan, The K/π ratio from condensed Polyakov loops, Phys. Rev. C **66**, 034903 (2002).
[47] W. j. Fu, Z. Zhang, and Y. x. Liu, $2+1$ flavor Polyakov-Nambu-Jona-Lasinio model at finite temperature and nonzero chemical potential, Phys. Rev. D **77**, 014006 (2008).
[48] P. Costa, M. C. Ruivo, C. A. de Sousa, H. Hansen, and W. M. Alberico, Scalar-pseudoscalar meson behavior and restoration of symmetries in SU(3) PNJL model, Phys. Rev. D **79**, 116003 (2009).
[49] C. A. Dominguez, L. A. Hernandez, and K. Schilcher, Determination of the gluon condensate from data in the charm-quark region, J. High Energy Phys. 07 (2015) 110.
[50] A. Pich and A. Rodríguez-Sánchez, Determination of the QCD coupling from ALEPH τ decay data, Phys. Rev. D **94**, 034027 (2016).
[51] A. Deur, S. J. Brodsky, and G. F. de Teramond, The QCD running coupling, Prog. Part. Nucl. Phys. **90**, 1 (2016).
[52] K. G. Chetyrkin and A. A. Pivovarov, Vacuum saturation hypothesis and QCD sum rules, Nuovo Cimento Soc. Ital. Fis. **100A**, 899 (1988).
[53] J. P. Carlomagno, D. G. Dumm, V. Pagura, and N. N. Scoccola, Meson phenomenology and phase transitions in nonlocal chiral quark models, J. Phys. Conf. Ser. **630**, 012049 (2015).
[54] L. McLerran and R. D. Pisarski, Phases of cold, dense quarks at large N(c), Nucl. Phys. **A796**, 83 (2007).
[55] L. McLerran, K. Redlich, and C. Sasaki, Quarkyonic matter and chiral symmetry breaking, Nucl. Phys. **A824**, 86 (2009).
[56] H. Abuki, R. Anglani, R. Gatto, G. Nardulli, and M. Ruggieri, Chiral crossover, deconfinement and quarkyonic matter within a Nambu-Jona Lasinio model with the Polyakov loop, Phys. Rev. D **78**, 034034 (2008).